CHAPTER
NINE

THERMAL INTERACTIONS BETWEEN BLOOD AND TISSUE: DEVELOPMENT OF A THEORETICAL APPROACH IN PREDICTING BODY TEMPERATURE DURING BLOOD COOLING/REWARMING

L. Zhu
T. Schappeler
C. Cordero-Tumangday
A. J. Rosengart

1 INTRODUCTION

The human thermoregulatory system is capable of maintaining body core temperature near 37°C over a wide range of environmental conditions and during exercise. This is largely facilitated by the vascular system of the body. In addition to its primary functions of mass transport of body metabolisms and regulation of systemic blood pressure, the human vascular system plays an important role in systemic thermoregulation. The blood, which can be viewed as the heat transport medium contained within the vasculature, exerts a duel influence on the thermal energy balance within the body. It acts both as a source or sink of thermal energy by redistributing and balancing the temperature differences between the arterial blood and the individual organ tissue. This dynamic tissue heat transfer is fundamental as some body organs give rise to abundant amounts of heat during exercise (i.e., muscles), whereas others are vitally dependent on nutrient supply (i.e., brain). Further, heat redistribution is life saving during changing environmental conditions, as in warming of the body during exposure to cold, or it can be disadvantageous, for example, by counteracting therapeutic temperature elevations for cancer treatment with increased blood perfusion of the target region.

To maintain a normal, or euthermic, body temperature, the vasculature facilitates the redistribution and transfer of heat throughout the body preserving a steady core temperature for all vital organs and making the human body relatively insensitive to environmental temperature changes. Theoretical calculations have shown that if the body would solely depend on heat conduction and not utilize blood-induced heat redistribution, the body would reach its steady state temperature at about 80°C [1], which, of course, is incompatible with survival. Heat redistribution and the consistency of an euthermic core temperature of 37°C rely on two main mechanisms. First, adjustments in cardiac output or blood recirculation time induced by central and local thermoregulatory responses allow rapid changes in heat 'turn over', and second, regulation of blood perfusion of the body surface and the skin and subcutaneous tissue permit both enhanced evaporative loss or preservation of heat as demanded by internal and external environmental temperature changes. If those compensatory mechanisms are exhausted, such as in heat stroke, the body experiences a critical decline in its ability to regulate temperature and will decompensate if not treated. The clinical implications of thermoregulatory failure are easily underscored by the fact that, despite aggressive medical care, about 25% of patients with heat stroke victims experience organ failure and 7-14% permanent neurological deficits [2].

Active control of body temperature is increasingly employed therapeutically in several clinical scenarios, most commonly to protect the brain from the consequences of either primary (i.e., head trauma, stroke) or secondary injury (i.e., after cardiac arrest with brain hypoperfusion). Mild to moderate hypothermia, during which brain temperature is reduced to 30 to 35°C, has been studied, among others, as an adjunct treatment for protection from cerebral ischemia during cardiac bypass injury [3], carotid endarterectomy [4], and resection of aneurysms [5] and it is also commonly employed in massive stroke and traumatic brain injury patients [6-7]. Even minute reductions in brain temperature as small as 1°C and importantly, the avoidance of any hyperthermia, can substantially reduced ischemic cell damage [8-9] and improve outcome [10]. Some of the beneficial effects of brain hypothermia include decrease in cerebral edema formation and intracranial pressures, reduction of tissue oxygen demands [11], and amelioration of numerous deleterious cellular biochemical mechanisms, including calcium shift, excitotoxicity, lipid peroxidation and other free-radical reaction [12].

Introduction of brain hypothermia is induced via whole body (systemic) cooling as currently no efficient and safe cooling device for targeted, selective brain cooling exists, although novel approaches and investigations are ongoing [13]. To achieve systemic cooling many methods have been advocated and

demonstrated various clinical success. Current strategies are either relatively safe but only modestly effective (e.g. antipyretics [14-15]; blankets, garments [16], peripheral infusion of a coolant [17]), or more effective in temperature reductions but invasive and elaborate such as endovascular cooling or extracorporeal heat exchange [18-19]. Unfortunately, practical limitations in procedural accessibility and nursing care availability often prohibit the use of more complicated and invasive fever reduction methods, highlighting the ongoing need for safer, simpler, and cost-effective cooling strategies. In clinical practice, the most effective way to control the temperature in critically ill patients is to directly cool the blood of major veins using intravascular cooling catheters [20]. Cooling rates as high as 5°C/hour can be achieved depending on the cooling capacity of the device and the patient's cooling response [19, 21-23].

The effect of blood flow on heat transfer in living tissue has been addressed previously [1] and, because of the complex geometry of the vascular system, two theoretical approaches are currently used to assess the blood flow effects in biological systems. First, vascular models which consider blood vessels as rigid tubes incorporated in organ tissues. However, despite the availability of detailed information on vascular geometry only several large blood vessels are generally considered in these models, neglecting the remaining vascular tree in order to reduce the complexity. Nevertheless, with the advance of computational techniques in recent years, models simulating more complex vascular networks have progressed rapidly and already demonstrated great potentials in accurate and point-to-point blood and tissue temperature mapping [24]. Second, an approach different from modeling the vasculature evaluates flow effects in biological systems is employed in continuum models which average the influence of flow and temperature on a controlled blood and tissue volume. Thus, in the considered tissue region the blood flow effect is treated by either adding an additional term or changing some of the thermophysical parameters in the traditional heat conduction equation. The continuum models are simple to use as long as one or two representative parameters related to blood flow are available. The limitation of the continuum models is their inability of mapping point-to-point temperature variation along blood vessels. The two most widely employed equations are the Pennes bioheat equation [25] and the Weinbaum-Jiji equation [26]. In the Pennes bioheat equation, blood flow effect is modeled as a source term and its strength is proportional to the local blood perfusion rate and the temperature difference between blood and tissue. In the Weinbaum-Jiji equation blood flow is modeled as an enhancement in tissue thermal conductivity. In the Pennes equation blood temperature is considered to be the same as the body core temperature; in the Weinbaum-Jiji equation, on the other hand, the effect of the blood temperature serves as the boundary condition of the tissue domain. As outlined above, due to

the complexity of the vasculature continuum models appear more favorable in simulating the temperature field of the human body. In either continuum model (Pennes or Weinbaum-Jiji), blood temperature is an input to the governing equation of the tissue temperature. However, in situations in which the blood temperature is actively lowered or increased both continuum models seem less adequate to account for the tissue-blood thermal interactions and to accurately predict the expected body temperature changes.

In this study, we developed a new simple theoretical model to study blood-tissue thermal interaction in the human body. In addition to using the Pennes bioheat equation to simulate the body temperature distribution during blood cooling/remarming, a heat transfer equation for the blood temperature was developed to account for the energy balance among blood and tissue as well as for the influence of external cooling or rewarming. The theoretical approach provided the solution procedures of solving for both the body and blood temperatures during active blood temperature modifications. A sample calculation of the body temperature transient was conducted using the theoretical approach to show its feasibility and accuracy. So far, the response pattern of an individual patient to manipulations of systemic temperature changes, such as vascular cooling or rewarming using intravenous fluids or endovascular catheters, has not been well delineated in the literature. A theoretical model simulating the cooling/rewarming process and temperature interactions between the blood and tissue (organs), as presented in this study, will help predict precisely these changes and is, therefore, of both clinical and scientific importance.

2 MATHEMATICAL FORMULATION

The mathematical formulation consists of simulation of both body temperature distribution and energy balance of the blood compartment of the body. The Pennes bioheat equation is used to simulate the body temperature, while a lumped system analysis is implemented to predict temperature change of the blood during clinical applications.

2.1 Body Temperature Distribution

The human body can be modeled as a simple cylinder or a combination of components representing torso, head, and limbs. As shown in Figure 1, the body is exposed to evaporation, convection, and radiation heat transfer on the skin surface. The Pennes bioheat equation simplifies the vasculature by modeling blood flow as a source term. The metabolism is considered as a heat source

within the body tissue and the blood perfusion in tissue is modeled as a heat source or sink depending on whether the arterial temperature is higher or lower than the local tissue temperature. The governing equation for the temperature field in the body tissue can be written as

$$\rho c \frac{\partial T_t}{\partial t} = k_t \nabla^2 T_t + q_m + \rho c \omega (T_a - T_t) \qquad (1)$$

where T_t is the body tissue temperature, ρ is density, c is specific heat, k_t is thermal conductivity of tissue, q_m is the volumetric heat generation rate (W/m^3) due to metabolism and ω is the local blood perfusion rate. The above governing equation can be solved once the boundary conditions and initial condition are prescribed. The boundary at the skin surface is modeled as a convection boundary subject to an environment temperature of T_{air} and a convection coefficient of h. h can be considered as the overall heat transfer coefficient related to the combined thermal resistance due to convection, radiation, evaporation at the skin surface. The Pennes bioheat equation has been used extensively in the past to model tissue temperature field for various clinical applications and has been considered as an accurate description of tissue temperature field.

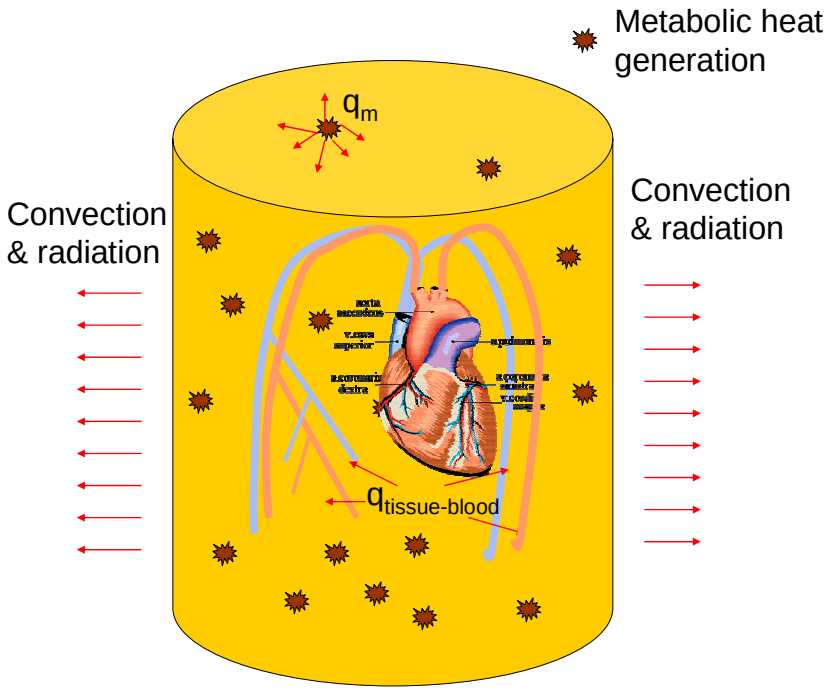

Figure 1. Schematic diagram of thermal interaction among tissue, blood, and environment.

We would like to emphasize that in Eq. (1), the arterial temperature T_a is used as an input. To predict the body temperature response to change of the arterial blood temperature during clinical applications, one needs to understand thermal interaction between blood and tissue. Unfortunately, Pennes equation alone would not predict the thermal interaction. In this study, we will analyze steady state temperature distribution and predict the overall energy balance of tissue-blood heat exchange.

Blood interaction with tissue is described by the Pennes perfusion source term (the third term on the right side of Eq. (1)). Depending on the local tissue temperature, it may act as either a heat source or a heat sink to tissue during circulation. Let's consider that in a steady state situation, the body can maintain stable body temperature and blood temperature. Maintaining a stable blood temperature implies that the total heat transfer between the blood and tissue should be equal to zero during steady state. It is suggested that heat loss from blood to tissue in the periphery tissue region would be compensated by the heat gain in the central region. Based on the Pennes bioheat equation, the rate of the total heat loss from the blood to tissue during steady state is

$$Q_{blood-tissue,0} = \iiint_{body\ volume} \rho c \omega (T_{a0} - T_{t0}) dV_{body} = \rho c \overline{\omega} (T_{a0} - \overline{T}_{t0}) V_{body} = 0 \qquad (2)$$

where subscript 0 represents steady state, V_{body} is the body volume, and $\overline{\omega}$ is the volumetric average blood perfusion rate defined as

$$\overline{\omega} = \iiint_{body\ volume} \omega \, dV_{body} \qquad (3)$$

$\overline{T_t}$ is the weighted average tissue temperature defined by Eq. (2) and is given by

$$\rho c \overline{\omega} (T_{a0} - \overline{T}_t) V_{body} = \iiint_{body\ volume} \rho c \omega (T_{a0} - T_{t0}) dV_{body} \qquad (4)$$

Note that $\overline{T_t}$ may not be equal to the volumetric average tissue temperature (T_{avg}) if ω is not uniform in the body tissue. Eq. (2) implies that during steady state the arterial blood temperature, T_a, should be the same as the weighted average tissue temperature, $\overline{T_t}$. The average body temperature $\overline{T_t}$ can be predicted by solving Eq. (1) and calculated by Eq. (4). During steady state thermal regulation in the human body ensures the energy balance to maintain stable body and blood temperatures. In this study we assume that the body maintains its steady state temperature via adjusting the convection coefficient on the skin surface.

However, during a transient heat transfer process such as blood cooling/rewarming, the rate of the total heat loss from blood to tissue is no longer equal to zero, and is given by

$$Q_{blood-tissue}(t) = \iiint_{body\ volume} \rho c \omega (T_a(t) - T_t(r,t)) dV_{body} = \rho c \overline{\omega} \left[T_a(t) - \overline{T}_t(t) \right] V_{body} \neq 0 \quad (5)$$

2.2 Energy Balance in Blood

During clinical applications, external heating or cooling of the blood can be implemented to manipulate the body temperature. Because of the relatively short recirculation time, blood in the human body is represented as a lumped system. We assume that a typical value of the blood volume of body, V_{blood}, is approximately 5 liters. A mathematical expression of the energy absorbed or removed per unit time is determined by the temperature change of the blood, and is written as:

$$\rho_{blood} c_{blood} V_{blood} \left[T_a(t + \Delta t) - T_a(t) \right] / \Delta t \approx \rho_{blood} c_{blood} V_{blood} \frac{dT_a}{dt} \qquad (6)$$

where $T_b(t)$ is the blood temperature at time, t, and $T_b(t+\Delta t)$ is at time $t+\Delta t$; ρ_{blood} is the blood density (kg/m^3), and c_{blood} (J/kg°C) is the specific heat of blood that measures the energy (J) needed to raise or decrease the temperature of 1 kg blood by 1°C. In the mathematical model, we propose that energy change in blood is due to the energy added or removed by external heating or cooling (Q_{ext}), and heat loss to the body tissue in the systemic circulation ($Q_{blood\text{-}tissue}$). Therefore, the governing equation for the blood temperature can be written as

$$\begin{aligned} \rho_{blood} c_{blood} V_{blood} \frac{dT_a}{dt} &= Q_{ext}(T_a) - Q_{blood-tissue}(t) \\ &= Q_{ext}(T_a) - \rho c \overline{\omega} V_{body} (T_a - \overline{T}_t) \end{aligned} \qquad (7)$$

where Q_{ext} may be a function of the blood temperature due to thermal interaction between blood and the external cooling approach, T_a, $\overline{T_t}$, $\overline{\omega}$, and Q_{ext} can be a function of time. Eq. (7) cannot be solved alone since $\overline{T_t}$ is determined by solving the Pennes bioheat equation. One needs to solve Eqs. (1) and (7) simultaneously.

2.3 Numerical Method of Solving Eq. (7)

The governing equation of the blood is a first order ordinary differential equation and can be solved numerically since most of the parameters in Eq. (7) are a function of time and solving for the blood temperature depends on solving for the whole body temperature field. The time derivative on the left side of Eq. (7) is discretized using finite difference form. Although either implicit or explicit method can be used, an undesirable feature of the explicit method is that it imposes a restriction on the time step to avoid oscillation in the solution, which is physically impossible. In this study, Eq. 7 is discretized using either the implicit scheme or the explicit scheme as follows:

$$implicit: \quad \rho_{blood} c_{blood} V_{blood} \frac{T_a^{P+1} - T_a^P}{\Delta t} = Q_{ext}(T_a^{P+1}) - \rho c \bar{\omega} V_{body}(T_a^{P+1} - \bar{T}_t^P) \quad (8a)$$

$$\exp licit: \quad \rho_{blood} c_{blood} V_{blood} \frac{T_a^{P+1} - T_a^P}{\Delta t} = Q_{ext}(T_a^P) - \rho c \bar{\omega} V_{body}(T_a^P - \bar{T}_t^P) \quad (8b)$$

where Δt is the time interval for solving for the transient blood temperature, and the superscript P denotes the time dependence of temperature. Superscript P and $P+1$ represent temperatures associated with the previous and new times, respectively. Note that Eqs. (8a) and (8b) are the discretized equation of T_a only, the new ($P+1$) blood temperature can be easily determined by re-arranging the equation. The finite element method (FEMLAB®) is used to solve Eq. (1) for the body temperature distribution. The following procedures are the general approach implemented in solving Eqs. (1) and (8).

1) Select a proper temperature of blood, T_{b0}, as the input to the Pennes bioheat equation. Use the FEMLAB® software to solve for the steady state temperature field of the body before the clinical treatment. Adjust the overall heat transfer coefficient h so that the blood temperature T_{a0} is equal to the weighted average body temperature $\bar{T}_{t0}$. The steady state temperature field (T_{a0} and $\bar{T}_{t0}$) serves as the initial temperature field of the transient heat transfer process.

2) Substitute the initial temperature values (time step P) into Eq. (8) and determine the blood temperature at the next time step ($P+1$).

3) The newly determined blood temperature at time step $P+1$ is then used as the input to the Pennes bioheat equation to solve for $\bar{T}_t^P$.

4) Steps 2 and 3 are repeated to solve for the transient temperature field of the subsequent time steps.

3 RESULTS

In this sample calculation, we apply the model to a blood cooling application, during which coolant is pumped into the inner tube of a catheter inserted into the femoral vein and advanced to the veno-vera. Once the coolant reaches the catheter, it flows back from the outer layer of the catheter and out of the cooling device. This cooling device has been used in clinical trials in recent years as an effective approach to decrease the temperature of the body for stroke or head injury patients. Based on previous research of this device, the cooling capacity of the device is around 100 W.

All the finite element calculations including the finite element mesh generation for Eq. (1) were performed on FEMLAB 3.1, operated on a Pentium IV processor of 2.79 GHz speed, using 1 GB of memory under a Windows XP SP2 Professional Operating System. The numerical model was obtained by applying the Galerkian formulation to Eq. (1). The total number of tetrahedral elements of the finite element mesh was around 135,000. The time dependent problem was solved using an adaptive time stepping scheme wherein the convergence criterion was kept at 10^{-6}. Mesh independency was checked by increasing the number of elements in the calculation domain by 100% over the current mesh. The finer mesh showed less than 1% difference in the temperature field. The CPU time for calculating each time step (Δt=60 seconds) is approximately 8 minutes.

A typical human body (male) has a body weight of 81 kg and 0.07421 m^3. We consider two body geometries and test whether the developed model yields similar results. As shown in Figure 2, the body can be modeled as a simple cylinder of 0.232 m in diameter and 1.8 m tall. A more realistic body geometry is illustrated by Figure 3, where the body consists of limbs, torso (internal organs and muscle), neck, and head. The green, red, and yellow color represents muscle, brain tissue, and internal organs, respectively. The limbs and neck are modeled as cylinders consisting of muscle. Note that the body geometry can be modeled more realistically if one includes a skin layer and a fat layer in each compartment. However, since our objective is to illustrate the principle and feasibility of the developed model, those details are neglected in the sample calculation. The simple geometry results in a body surface area of 1.312 m^2, while the detailed geometry has a body surface area of 1.8 m^2. Based on a previous study by Mosteller [27], the body surface area is usually calculated by the following formula:

$$surface\ area = \sqrt{[height\ (cm)\ x\ weight\ (kg)]/3600} \quad (9)$$

For a realistic human body with a body weight of 81 kg and 0.07421 m^3, the calculated body surface area based on Eq. (9) is around 2.012 m^2. The detailed body geometry used in this study agrees relatively well with the realistic body surface area. Table 1 gives the geometrical parameters used in both models.

Table 1. Geometrical parameters used in both models

	Simple Geometry	Detailed Geometry
Height (m)	1.8	1.8
Radius (m)	0.232	---
Head volume (m^3)	n/a	0.004206
Neck volume (m^3)		0.001287
Internal organ volume (m^3)		0.019503
Torso (w/o internal organ) volume (m^3)		0.019406
Upper arm volume (each) (m^3)		0.002085
Lower arm volume (each) (m^3)		0.001622
Upper leg volume (each) (m^3)		0.00695
Lower leg volume (each) (m^3)		0.005212
Total volume V_{body} (m^3)	0.0761424	0.076142
Total blood volume V_{blood} (m^3)	0.005	0.005
Total weight m_{body} (kg)	80.7	80.7

Table 2. Physical and physiological parameters used in both models.

		Simple Geometry	Detailed Geometry
Thermal conductivity k		0.5 W/m°C	0.5 W/m°C
Density ρ		1060 kg/m^3	1060 kg/m^3
Specific heat c		3800 J/kg°C	3800 J/kg°C
Blood perfusion rate ω	Muscle	0.0001129 (1/s)	0.0005 (1/s)
	Head	n/a	0.0083333 (1/s)
	Internal organ	n/a	0.001266 (1/s)
Metabolic heat generation rate q_m	Muscle	1249.7 W/m^3	553.5 W/m^3
	Head	n/a	9225 W/m^3
	Internal organ	n/a	1401.5 W/m^3

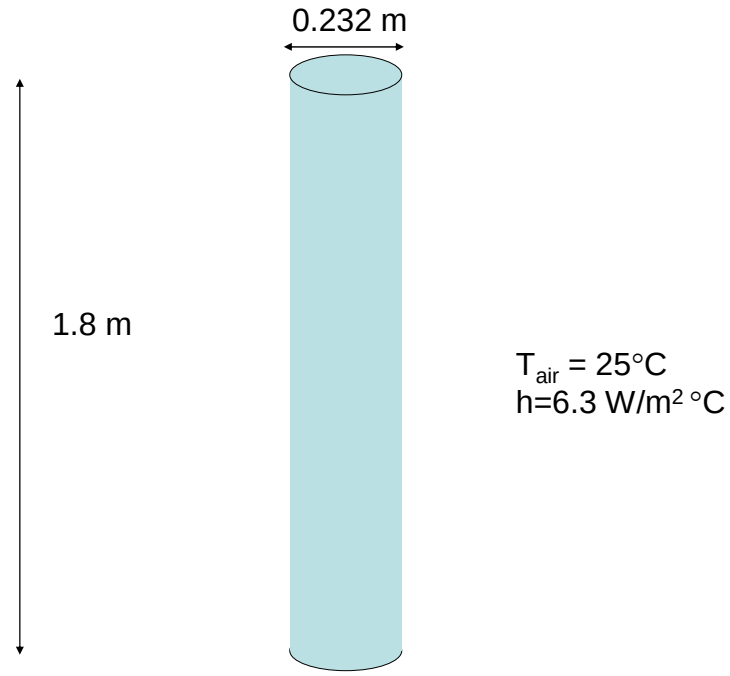

Figure 2. Schematic diagram of a simplified human body geometry.

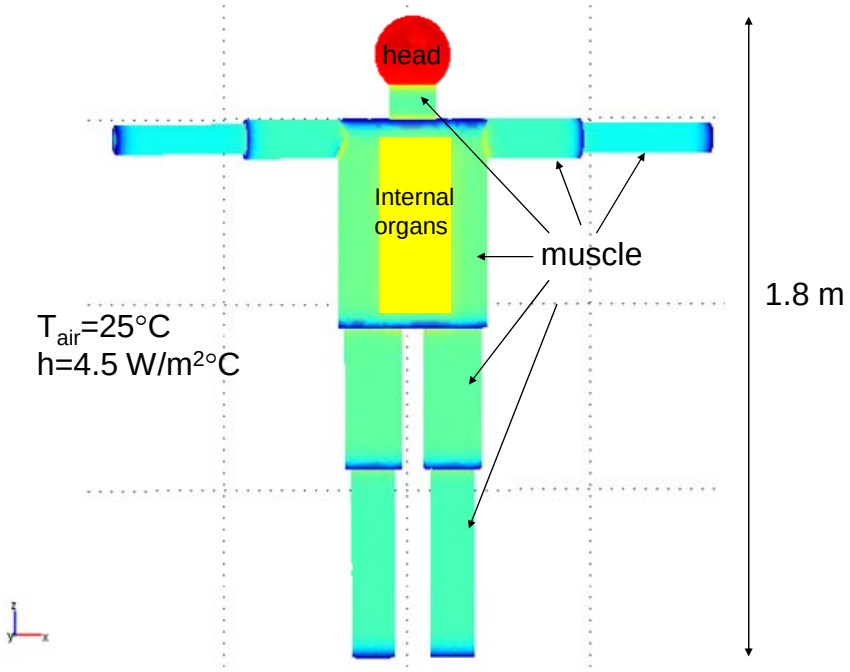

Figure 3. Schematic diagram of the detailed human body geometry.

The average stroke volume is 0.7 liter and heart beat is 75 beats/min. Based on the total body mass of 81 kg, one can determine the average blood perfusion rate as 6.773 ml/min.100g tissue or 0.001129 (s^{-1}). For the simple one compartment model, the average metabolic heat generation rate is estimated based on a food consumption of 2000 kCal/day and is equal to 1250 W/m^3. The metabolic heat generation rate and local blood perfusion rate used in the detailed body model are listed in Table 2.

The body is exposed to an evaporation, convection, and radiation environment with an overall heat transfer coefficient h and a room temperature of 25°C. The clothes covering the human subject can be modeled as a thermal resistance and incorporated into the overall heat transfer coefficient h. In this sample calculation, ω, h and T_{air} are assumed unchanged during the cooling process. The initial blood temperature is assigned as 37°C.

Temperature field in the simplified human body can be considered as three-dimensional and the steady state temperature can be determined by the FEMLAB® software using the finite element method. During steady state, the convection heat transfer coefficient h is adjusted to 6.3 W/m^2 °C and 4.7 W/m^2 °C for the simple and detailed models, respectively, so that the average body temperature $\overline{T}_{t0}$ is equal to the blood temperature T_{a0}. The different values of h used in those two models can be explained by the different body surface areas. From the energy balance of the entire body during steady state, the metabolic heat generation inside the body has to be dissipated from the body surface via convection and radiation. Figure 4 shows the steady state temperature distribution in the body ranging from 37.275°C inside the brain to 34°C at the finger tip. The left image of the temperature contours are the temperature distribution using the simple geometry. The maximum body temperature is usually slightly higher than the arterial temperature due to metabolic heat generation. The maximum temperature usually occurs inside the brain tissue due to its large metabolic heat generation rate. Note that the detailed body geometry gives a more realistic temperature contours in the body, while the simple model still correctly predicts the maximum and minimum temperatures in tissue. The simulated steady state temperature distribution is used as the initial temperature field for the simulation of the transient heat transfer process.

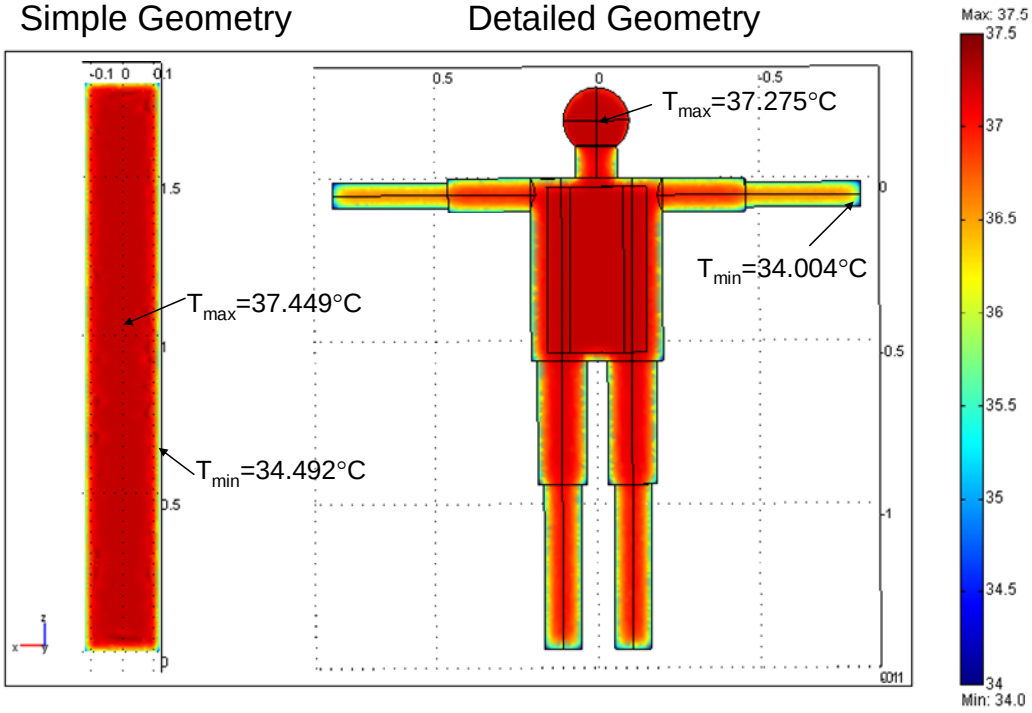

Figure 4. Initial steady state temperature contours of the human body.

Since the cooling capacity of the cooling device is around 100 W, one models the external cooling to the blood Q_{ext} as -100 W. One can rewrite the discretized equation for T_a using the explicit scheme as follows:

$$T_a^{P+1} = T_a^P\left(1-\frac{\rho c\bar{\omega}V_{body}\Delta t}{\rho_{blood}c_{blood}V_{blood}}\right)+\frac{Q_{ext}\Delta t}{\rho_{blood}c_{blood}V_{blood}}+\bar{T}_t^P\left(\frac{\rho c\bar{\omega}V_{body}\Delta t}{\rho_{blood}c_{blood}V_{blood}}\right) \quad (9)$$

Note that the coefficient of the first term on the right side of Eq. (9) has to be positive to avoid oscillation of the solution. This restriction requires

$$1-\frac{\rho c\bar{\omega}V_{body}\Delta t}{\rho_{blood}c_{blood}V_{blood}} \geq 0 \quad or \quad \Delta t \leq \frac{\rho_{blood}c_{blood}V_{blood}}{\rho c\bar{\omega}V_{body}} \quad (10)$$

In this sample calculation, Δt is selected as 60 seconds, which satisfies the constraint in Eq. (10).

The discretized equation for T_a using the implicit scheme can be written as

$$T_a^{P+1} = \frac{\dfrac{Q_{ext}\Delta t}{\rho_{blood} c_{blood} V_{blood}} + T_a^P + \bar{T}_t^P \left(\dfrac{\rho c \bar{\omega} V_{body} \Delta t}{\rho_{blood} c_{blood} V_{blood}} \right)}{\left(1 + \dfrac{\rho c \bar{\omega} V_{body} \Delta t}{\rho_{blood} c_{blood} V_{blood}} \right)} \qquad (11)$$

The time step is also selected as 60 seconds.

Figure 5 shows the simulated temperature of the arterial blood during the first 20 minutes of the cooling. The observed difference between the implicit and explicit schemes used in both body geometries suggests that the time step should be selected smaller than 60 seconds to minimize the error associated with the approximation of the time derivative in the numerical method. Up to 0.737°C decrease in the arterial temperature is achieved during the first 20 minutes using the implicit scheme. One notices the large initial temperature drop and the temperature decay rate is slowed down and stable at approximately 0.019°C/min in the detailed model. Based on the cooling rate, it is expected that the arterial blood temperature will decrease to 35.5°C after one hour and 34.4°C after two hours.

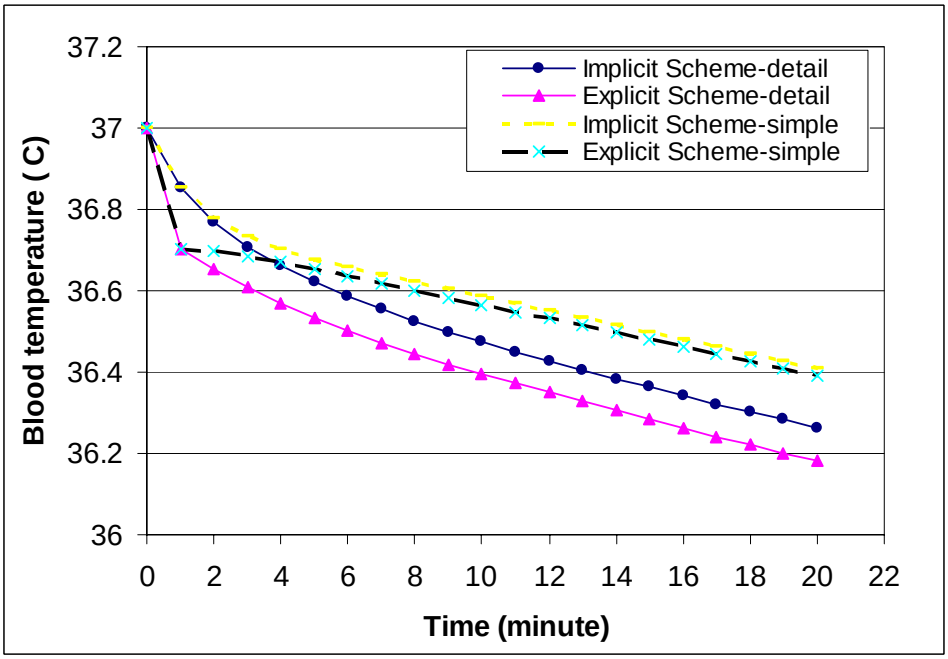

Figure 5. Simulated blood temperature changes during the cooling using both implicit and explicit schemes.

In clinical applications of whole body cooling for stroke or head injury patients, physicians are more interested in the temperature of the body tissue. The maximum tissue temperature, the minimum tissue temperature at the skin surface, the volumetric average body temperature (T_{avg}), and the weighted average body temperature ($\overline{T_t}$) are plotted in Figure 6. The difference between the volumetric average body temperature and the weighted average body temperature is due to their different definitions. All tissue temperatures decrease almost linearly with time and after 20 minutes the cooling results in approximately 0.3~0.5°C tissue temperature drop. The cooling rate of the skin temperature is smaller (0.2°C per 20 min). As shown in Figure 7a, the initial cooling rate of the blood temperature in the detailed model is very high (~ 0.14°C/min) and then it decreases gradually until it is stabilized after approximately 20 minutes. On the other hand, cooling the entire body (the volumetric average body temperature) starts slowly and gradually catches up. It may be due to the inertia of the body mass in responding to the cooling of the blood. Figure 7a also illustrates that after the initial fluctuation, the stabilized cooling rates of all temperatures approach each other and they are approximately 0.019°C/min or 1.15°C/hour. The cooling rates of all temperatures in the simple model are plotted in Figure 7b, where the cooling rates converge to approximately 0.018°C/min only after 10 minutes. The simulated results demonstrate the feasibility of inducing mild body hypothermia (34°C) within three hours using the cooling approach.

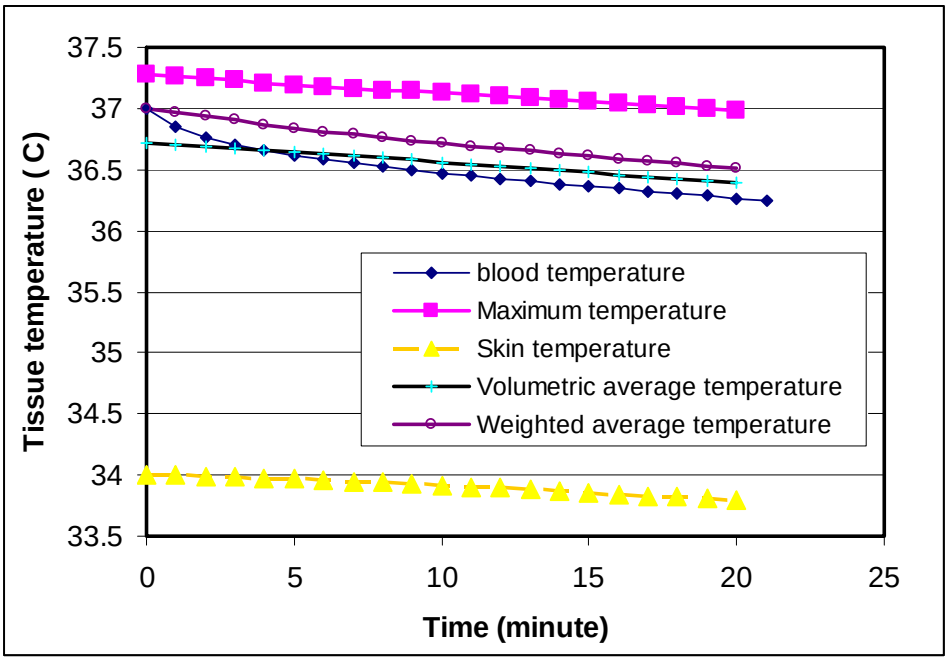

Figure 6. Temperature decays during the cooling process using the detailed geometry and implicit scheme.

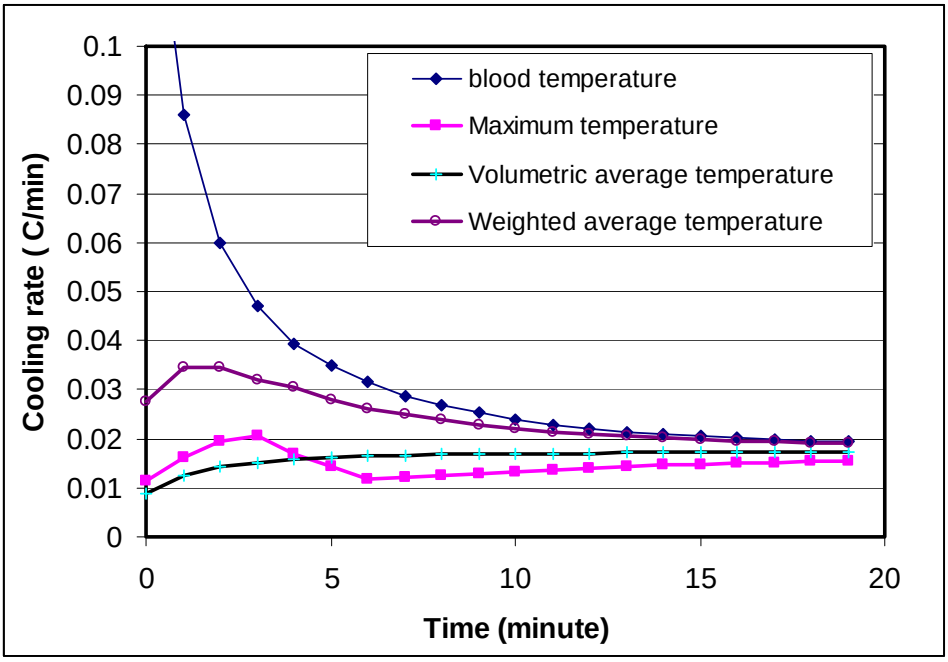

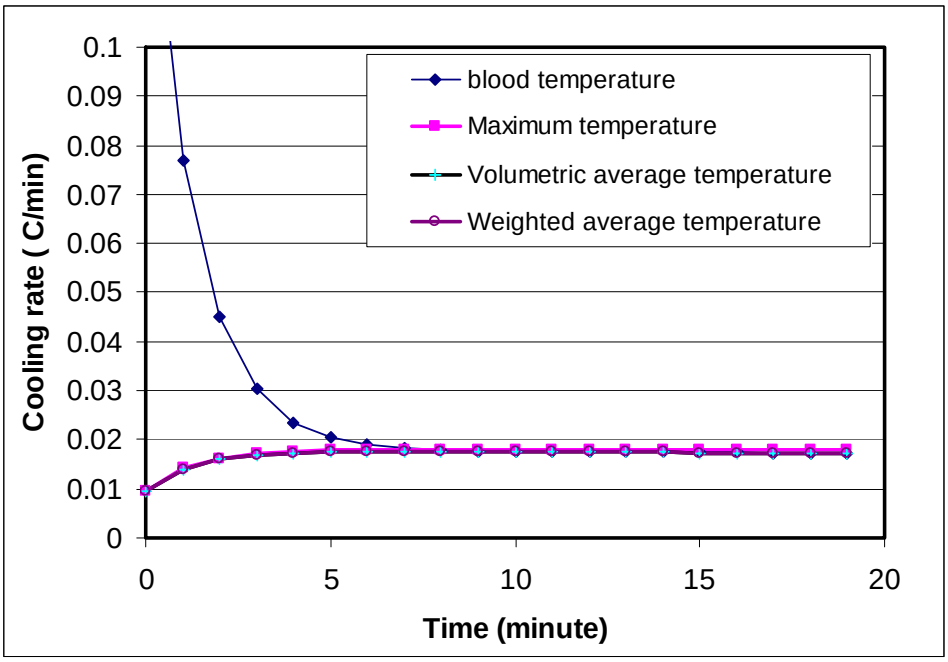

Figure 7. Induced cooling rates of the blood temperature, the maximum temperature, the volumetric average temperature, and the weighted average temperature. (a) the detailed model and (b) the simple model.

The first term on the right side of Eq. (8) represents the external cooling rate if the blood does not gain heat from the tissue. It is estimated that the cooling rate induced by this term is approximately equal to 18.9°C/hour, which is much higher than the achieved cooling rate of the body. It is understandable since the cooling capacity induced by the external cooling device cools not only the blood, but also the entire body. Therefore, the second term on the right side of Eq. (8) representing blood-tissue thermal exchange is mainly dependent on the temperature difference between the blood and tissue. During blood cooling, blood is colder than the average body temperature, therefore, the second term on the right side of Eq. (8) is positive to account for the heat transfer from the tissue to the blood. One notices that the initial temperature difference is zero since the thermal balance is established during the initial steady state (Eq. (2)). Later, the temperature difference changes and becomes stabilized as -2.5°C. After the difference between T_a and $\overline{T_t}$ is stabilized (approximately 20 minutes after the initiation of the cooling), the right side of Eq. (8) becomes a constant. This is the direct result of the assumptions that the external cooling capacity (Q_{ext}), the metabolic heat generation rate, as well as all the physiological parameters such as the blood perfusion rate and convective coefficient are kept the same during the

cooling simulation. Once the temperature difference is unchanged, it is expected that the cooling rate of the blood temperature governed by Eq. (8) would become a constant. One can then extrapolate the current simulated data to later time duration.

The effect of simplification of the body geometry on the body temperature transients is illustrated in Figure 9. Implicit scheme is used with a time step of 60 seconds. Although the two geometries are quite different, the yielded cooling rates of the volumetric average body temperature (T_{avg}) during the cooling are very similar. Both geometries have the same body weight and volume. The results imply that it is the overall energy balance that determines the temperature reduction of the body tissue. The limitation of the simple model lies in its inability of modeling any realistic thermal regulation during the cooling process.

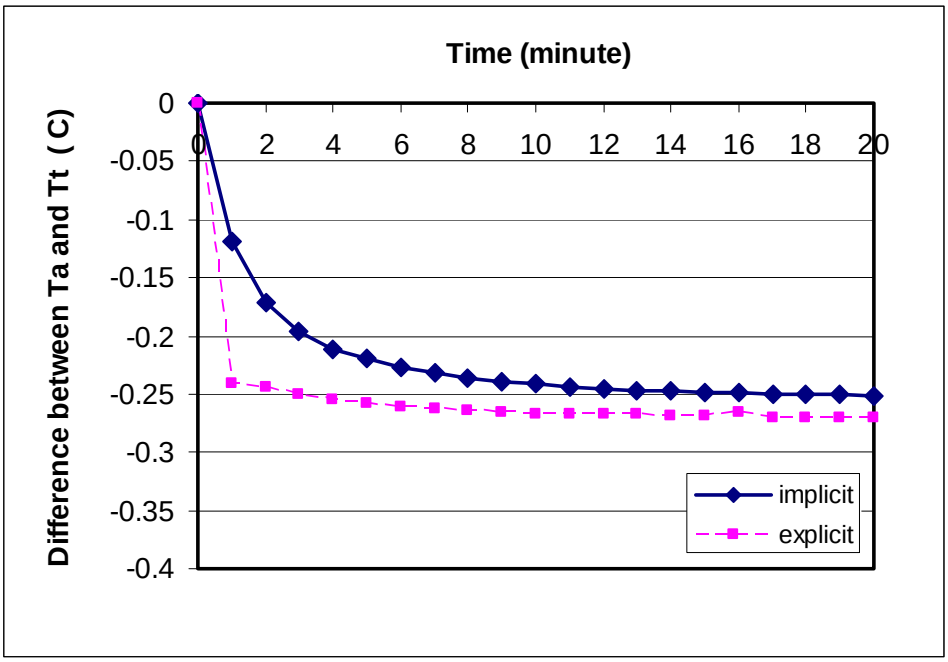

Figure 8. Difference between the blood temperature and the weighted average body temperature during cooling.

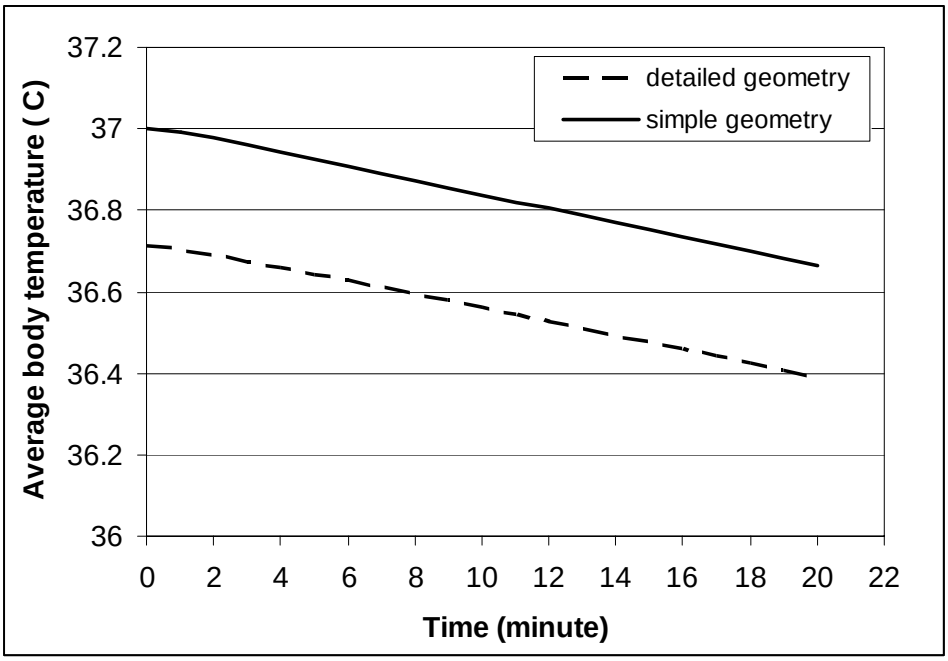

Figure 9. The effect of model geometry on the volumetric average body temperature.

4. DISCUSSION

The provided sample calculations identified the feasibility of applying the model for predicting the temperature distribution in the human body during blood cooling and rewarming. The accuracy of the model can be confirmed by comparing the predicted results from the model to that using a simple lumped analysis of the whole body induced by an external, intravascular cooling device with a capacity of 100 W as estimated by the following equation:

$$\text{Cooling rate} = -100 /(\rho V_{body}\, c) = -100/(1060 \times 0.076142 \times 3800) \quad (12)$$
$$= 3.2605 \times 10^{-4}\ ^{\circ}\text{C/second} = 0.0196^{\circ}\text{C/min}$$

The estimated cooling rate is very close to the rate predicted by the developed model employing both the implicit and explicit schemes. Decreasing the time step would further improve the accuracy of the model, however, this would increase the CPU time.

The theoretical models developed by Wissler and other investigators [28-31] similarly introduced the whole body as a combination of multiple compartments. However, a major difference between the current model and previous approaches

is the assessment of the thermal interactions between the blood and tissue in each compartment. The majority of previously published studies introduced a pair of countercurrent artery and vein with their respective branching (flow system) and then modeled the temperature variations along this flow system to derive the heat transfer between the blood vessels and tissue within each flow segment. Such an approach is computationally intensive although the models are capable of delineating the temperature decay along the artery and the rewarming by the countercurrent vein. The modeling approach introduced here greatly simplifies the theoretical simulations, and therefore, requires less computational resources and time. In our approach, the vasculature is modeled as a lumped system only varying as a function of time and the blood-tissue thermal interactions are evaluated by integrating the Pennes perfusion source term over the entire body tissue. The reasoning for combining these modeling steps is based on two assumptions. First, several previous theoretical and experimental studies have suggested that the thermal equilibration length of the major supply artery is much longer than its physical length. This implies that the temperature of the arterial blood in each tissue compartment should be very close to the body core temperature. Second, we chose to neglect the rewarming effect by the venous blood due to countercurrent heat exchange. Although recent studies by the authors and others [32-33] suggested a 30% rewarming rate originating from the venous system and therefore, to multiply the Pennes perfusion source term by a correction coefficient of 0.7, there are currently no rigorously designed animal studies validating such theoretical reasoning. This lack of animal data originates mainly from the difficulty to measure with precision the local *in vivo* blood perfusion rate. Should, however, this correction coefficient value become experimentally verified and available, the Pennes perfusion term can easily be modified to also account for the effect of countercurrent venous rewarming in tissue. We feel the current model using the Pennes perfusion term and lumped system of the blood is simple to use in comparison with these previous whole body models while providing meaningful and accurate theoretical estimates.

The presented sample calculations suggest that the developed model is accurate in describing the overall thermal balance between blood and body tissue during clinical applications involving blood cooling. Recent animal and clinical studies have demonstrated the effectiveness of improving patient outcome inducing systemic cooling and/or actively avoiding hyperthermic (febrile) episodes after brain injury [34-39]. Controlling fever has become a more important clinical treatment task since it is known that more than 60% of brain injury victims developed fever within 72 hours and the three-month mortality rate in these patients is significantly higher than those who remained normothermic (1% vs. 15.8%, respectively) [40]. Theoretical models have suggested that the actual

cooling rate of the volumetric average body temperature depends largely on the cooling capacity of the cooling device. Among the currently utilized strategies for direct blood cooling are intravascular cooling by placing a cooling catheters within a larger veins of the trunk, or less invasively using a peripheral infusion scheme, the intravenous bolus infusion of saline with ice slurry [17, 41-42]. Based on these calculations and our clinical experience, a cooling capacity of 100 W delivered intravenously to a patient of average build will results in a ~1.2°C/hour cooling rate. For example, intravascular cooling can achieve within less than three hours systemic and hence, brain hypothermia of 34°C or, similarly, reduce critical fever of 40°C to euthermia temperatures. For instance, an intravenous cooling catheter manufactured by Innercool® can deliver a cooling capacity of up to 200 W (personal communication, August 2007) and therefore, is capable of rapid systemic cooling within even shorter time frames. As expected, the cooling capacity of intravenous infusion regimens is much smaller mainly due to limitations in the infusion rate and luminal diameter of quickly accessible, peripheral veins. Recent theoretical evaluations by our group suggest that the cooling capacity is approximately 40 W per hour when using 50% ice slurry at an infusion rate of 450 ml/hour [17]. Therefore, the cooling rate induced by intravenous infusion of 50% ice slurry/saline solutions can be extrapolated to be ~0.5°C/hour, less than half than that expected from a 100 W cooling catheter.

Another application of the developed and here proposed model involves the representation of the re-warming process, i.e., after induces systemic hypothermia or for the treatment for body hypothermia. Rapid rewarming in those applications may result in dangerous rebound intracranial pressure elevation and cerebral perfusion pressure reduction ultimately worsening outcome in brain injury. Several clinical investigations [41, 43] have emphasized the importance of gradual rewarming to minimize this clinical problem with rewarming. In support, a recent animal study performed by Diao and Zhu [44] suggested that a fast rewarming rate in normal hypothermic rats results in local blood perfusion-metabolism mismatch which may explain the clinical worsening observed in some patients exposed to accelerated rewarming. Conveniently, the current model can be applied to assist in the design of an optimal rewarming strategy for clinical practice. In a research paper published by our group [45], a theoretical model was developed to simulate targeted brain hypothermia induced by an interstitial cooling device in the human neck. This previous model can be combined with the whole body model for designing the temperature elevation strategy in the interstitial cooling device to achieve desired rewarming rates in both the body core and brain.

In the presented sample calculations we also found that the simple geometry model yields very similar cooling rates as those predicted by a more detailed model. However, the simple model is not capable of simulating blood redistribution in the body as local blood perfusion and/or metabolic heat generation rates are a function of the tissue location. Both models can be used in applications when the physiological parameters, such as local blood perfusion rate, metabolic heat generation rate, or environmental thermal conditions, vary during blood cooling or rewarming. Previous studies have shown that the temperature dependence of local blood perfusion is based on a coupled relationship between blood perfusion and metabolism. For example, it has been calculated that hypothermia decreases cerebral metabolic rate by an average value of 7% for the first 1°C reduction in temperature, while it is reduced by 50% of normal baseline when the temperature reduction approaches 10°C [46]. Our developed models are capable of including the dynamic responses of physiological parameters changes during the simulation.

Although the model was developed for applications involving blood cooling or rewarming, the detailed geometry can also be used to accurately predict the body temperature changes during exercise. It is well known that strenuous exercise increases cardiac output, redistributes blood flow from internal organs to muscle, increases metabolism in exercising muscle, and enhances heat transfer to the skin. Our detailed model can be easily modified to also include a skin layer and a fat layer in the compartments of the limbs. Further, redistribution of blood flow from the internal organs to the musculature can be modeled as changes of the local blood perfusion rate in the respective compartments and the enhanced skin heat transfer can be adjusted for by increasing the overall heat transfer coefficient (h). Therefore, one can use the detailed model to accurately delineate important clinical scenarios, such as heat stroke, and predict body temperature elevations during heavy exercise and/or heat exposures.

In summary, in this study a theoretical model is developed to simulate the transient body temperature distribution and blood temperature during blood cooling/rewarming. It is a relatively simple but accurate whole body model for an improved prediction of body temperature changes during various clinical scenarios and applications. The model's predictive strength has been demonstrated by sample calculations with intravascular cooling. With minor modifications, the detailed body geometry can be adjusted easily to also describe body temperature changes during physiological and medical conditions such as exercise or rewarming of a hypothermic patient.

NOMENCLATURE

c Specific heat capacity (J/kgK)
k Thermal conductivity (W/mK)
h Overall heat transfer coefficient (W/m^{2}K)
q_m Local metabolic heat generation rate (W/m^3)
t Time (s)
T Temperature (°C or K)
T_a Temperature of the blood (°C or K)
T_{avg} Volumetric average body temperature (°C or K)
T_{max} The maximum temperature in body tissue (°C or K)
T_t Tissue temperature (°C or K)
$\overline{T_t}$ Weighted average body temperature (°C or K)

Greek Symbols

ρ Density (kg/m^3)
ω Local blood perfusion rate (1/s)
$\overline{\omega}$ Volumetric average blood perfusion rate of the human body (1/s)

Subscript

a Artery
b Blood
m Metabolism
avg Average
t Tissue
0 Steady state or initial condition

REFERENCES

1. L. Zhu, Bioheat transfer. Chapter 2 in *Standard Handbook of Biomedical Engineering & Design*, pp.2.3-2.29, Myer Kutz, editor-in-chief, McGraw-Hill, 2002.
2. A. Bouchama, Heatstroke: a New Look at an Ancient Disease, *Intensive Care Medicine*, vol. 21, pp 623-625, 1995.
3. N. A. Nussmeier, A Review of Risk Factors for Adverse Neurological Outcome after Cardiac Surgery, *JECT*, vol.34, pp.4-10, 2002.
4. S. W. Jamieson, D. P. Kapelanski, N. Sakakibara, G. R. Manecke, P. A. Thistlethwaite, K. M. Kerr, R. N. Channick, P. F. Fedullo, and W. R. Auger, Pulmonary Endarterectomy: Experience and Lessons Learned in 1,500 Cases, *Ann. Thorac. Surg.*, vol.76(5), pp.1457-1462, 2003.

5. K. R. Wagner, and M. Zuccarello, Local Brain Hypothermia for Neuroprotection in Stroke Treatment and Aneurysm Repair, *Neurological Research*, vol.27, pp.238-245, 2005.
6. D. W. Marion, Y. Leonov, M. Ginsberg, L. M. Katz, P. M. Kochanek, A. Lechleuthner, E. M. Nemoto, W. Obrist, P. Safar, F. Sterz, S. A. Tisherman, R. J. White, F. Xiao, and H. Zar, Resuscitative Hypothermia, *Crit. Care Med.*, vol.24(2), pp.S81-S89, 1996.
7. D. W. Marion, L. E. Penrod, S. F. Kelsey, W. D. Obrist, P. M. Kochanek, A. M. Palmer, S. R. Wisniewski, and S. T. DeKosky, Treatment of Traumatic Brain Injury with Moderate Hypothermia, *N. Engl. J. Med.*, vol.336, pp.540-546, 1997.
8. R. S. Clark, P. M. Kochanek, D. W. Marion, J. K. Schiding, M. White, A. M. Palmer,, and S. T. DeKosky, Mild Posttraumatic Hypothermia Reduces Mortality after Severe Controlled Cortical Impact in Rats, *J. Cereb. Blood Flow Metab.*, vol:16(2), pp.253-261, 1996.
9. C. T. Wass, W. L. Lanier, R. E. Hofer, B. W. Scheithauer, and A.G. Andrews, Temperature Changes of ≥ 1°C Alter Functional Neurological Outcome and Histopathology in a Canine Model of Complete Cerebral Ischemia, *Anesthesia*, vol.83, pp.325-335, 1995.
10. J. Reith, H. S. Jorgensen, P. M. Pedersen, H. Nakayama, H. O. Raaschou, L. L. Jeppesen, T. S. Olsen, Body Temperature in Acute Stroke: Relation to Stroke Severity, Infarct Size, Mortality, and Outcome, *Lancet*, vol.347, pp.422-425, 1996.
11. U. M. Illievich, M. H. Zornow, K. T. Choi, M. S. Scheller, and M. A. Strnat, Effects of Hypothermic Metabolic Suppression on Hippocampal Glutamate Concentrations after Transient Global Cerebral Ischemia, *Anesth. Analg.*, vol.78(5), pp.905-911, 1994.
12. K. H. Polderman, Keeping a Cool Head: How to Induce and Maintain Hypothermia, *Crit. Care Med.*, vol.32(12), pp.2558-2560, 2004.
13. L. Zhu and A. J. Rosengart, Cooling Penetration into Normal and Injured Brain via Intraparenchymal Brain Cooling Probe: Theoretical Analyses. *Heat Transfer Engineering*, vol.28(3), 2008 (in press).
14. D. W. Dippel, E. J. van Breda, H. M. van Gemert, H. B. van der Worp, R. J. Meijer, L. J. Kappelle, P. J. Koudstaal, Effect of Paracetamol (Acetaminophen) on Body Temperature in Acute Ischemic Stroke: A Double-Blind, Randomized Phase II Clinical Trial, *Stroke*, vol.32, pp.1607-1612, 2001.
15. G. Sulter, J. W. Elting, N. Mauritus, G. J. Luyckx, J. De Keyser, Acetylsalicylic Acid an Dacetaminophen to Combat Elevated Body Temperature in Acute Ischemic Stroke, *Cerebrovascular Disease*, vol.17, pp.118-122, 2003.

16. S. Mayer, C. Commichau, N. Scarmeas, M. Presciutti, J. Bates, D. Copeland, Clinical Trial of an Air-Circulating Cooling Blanket for Fever Control in Critically Ill Neurological Patients, *Neurology*, vol.56, pp.292-298, 2001.
17. A. J. Rosengart, L. Zhu, T. Schappeler, and F. D. Goldenberg, Fever Control in Hospitalized Stroke Patients Using Simple Intravenous Fluid Regimens – A Theoretical Evaluation, *Journal of Clinical Neuroscience*, under review, 2007.
18. A. Piepgras, H. Roth, L. Schurer, R. Tillmans, M. Quintel, P. Herrmann, P. Schmiedek, Rapid Active Internal Core Cooling for Induction of Moderate Hypothermia in Head Injury by Use of an Extracorporeal Heat Exchanger, *Neurosurgery*, vol.42, pp.311-317, 1998.
19. A. G. Doufas, O. Akca, A. Barry, D. A. Petrusca, M. I. Suleman, N. Morioka, J. J. Guarnaschelli, D. I. Sessler, Initial Experience with a Novel Heat-Exchanging Catheter in Neurosurgical Patients, *Anesthesia and Analgesia*, vol.95, pp.1752-1756, 2002.
20. M. W. Dae, D.W. Gao, P. C. Ursell, C. A. Stillson, and D. I. Sessler, Safety and Efficacy of Endovascular Cooling and Re-Warming for Induction and Reversal of Hypothermia in Human-Sized Pigs, *Stroke,* vol. 34, pp.734-738, 2003.
21. D. Georgiadis, S. Schwarz, R. Kollmar, and S. Schwab, Endovascular Cooling for Moderate Hypothermia in Patients with Acute Stroke: First Results of a Novel Approach, *Stroke*, vol.32, pp.2550-2553, 2001.
22. B. Inderbitzen, S. Yon, J. Lasheras, J. Dobak, J. Perl, and G. K. Steinberg, Safety and Performance of a Novel Intravascular Catheter for Inducing and Reversal of Hypothermia in a Porcine Model, *Neurosurgery*, vol.50, pp.364-370, 2002.
23. W. J. Mack, J. Huang, C. Winfree, G. Kim, M. Oppermann, J. Dobak, B. Iderbitzen, S. Yon, S. Popilskis, J. Lasheras, R. R. Sciacca, D. J. Pinsky, and E. S. Connolly, Ultrarapid, Convection-Enhanced Intravascular Hypothermia: a Feasibility Study in Nonhuman Primate Stroke, *Stroke*, vol.34, pp.1994-1999, 2003.
24. B. W. Raaymakers, J. Crezee, and J. J. W. Lagendijk, Modeling Individual Temperature Profiles From An Isolated Perfused Bovine Tongue, *Phys. Med. Biol.*, vol.45, pp.765-780, 2000.
25. H. H. Pennes, Analysis of Tissue and Arterial Blood Temperatures in the Resting Human Forearm, *Journal of Applied Physiology*, vol.1, pp.93-122, 1948.
26. S. Weinbaum, and L. M. Jiji, A New Simplified Bioheat Equation for the Effect of Blood Flow on Local Average Tissue Temperature, ASME *Journal of Biomechanical Engineering*, vol.107, pp.131-139, 1985.

27. R. D. Mosteller, Simplified Calculation of Body Surface Area, *New England Journal of Medicine*, vol. 317, pp. 1098, 1994.
28. G. Fu, A Transient 3-D Mathematical Thermal Model for the Clothed Human, Ph.D. Dissertation, Kansas State University, 1995.
29. M. D. Salloum, A New Transient Bioheat Model of the Human Body and Its Integration to Clothing Models, M.S. Thesis, American University of Beirut, 2005.
30. C. E. Smith, A Transient Three-Dimensional Model of the Thermal System, Ph.D. Dissertation, Kansas State University, 1991.
31. E. H. Wissler, Mathematical Simulation of Human Thermal Behavior Using Whole Body Models, Heat and Mass Transfer in Medicine and Biology, Chapter 13, pp.325-373, New York: Plenum Press, 1985.
32. S. Weinbaum, L. X. Xu, L. Zhu, and A. Ekpene, A New Fundamental Bioheat Equation for Muscle Tissue, Part I: Blood Perfusion Term, ASME *Journal of Biomechanical Engineering*, vol.121, pp.1-12, 1997.
33. L. Zhu, L. X. Xu, Q. He, and S. Weinbaum, A New Fundamental Bioheat Equation for Muscle Tissue Part II: Temperature of SAV Vessels. ASME *Journal of Biomechanical Engineering*, vol.124, pp.121-132, 2002.
34. G. Azzimondi, L. Bassein, F. Nonino, L. Fiorani, L. Vignatelli and R. Re G. D'Alessandro, Fever in Acute Stroke Worsens Prognosis: A Prospective Study, *Stroke*, vol.26(11), pp.2040-43, 1995.
35. G. Boysen, and H. Christensen, Stroke Severity Determines Body Temperature in Acute Stroke, *Stroke*, vol.32(2), pp.413-17, 2001.
36. J. Castillo, F. Martinez, R. Leira, J. M. Prieto, M. Lema, and M. Noya, Mortality and Morbidity Of Acute Cerebral Infarction Related to Temperature and Basal Analytic Parameters, *Cerebrovasc*., vol.4, pp.56-71, 1994.
37. B. Hindfelt, The Prognostic Significance of Subfebrility and Fever in Ischaemic Cerebral Infarction, *Acta Neurologica Scandinavica*, vol.53(1), pp.72-79, 1976.
38. L. P. Kammersgaard, H. S. Jorgensen, J. A. Rungby, J. Reith, H. Nakayama, U. J. Weber, J. Houth, and T. S. Olsen, Admission Body Temperature Predicts Long-term Mortality after Acute Stroke: The Copenhagen Stroke Study, *Stroke*, vol.33(7), pp.1759-62, 2002.
39. A. Terent, and B. Anderson, Prognosis for Patients with Cerebrovascular Stroke and Transient Ischemic Attacks, *Journal of Med. Science*, vol.86(1), pp.63-74, 1981.
40. J. Castillo, A. Davalos, J. Marrugat, and M. Noya, Timing for Fever-Related Brain Damage in Acute Ischemic Stroke, *Stroke*, vol.29(12), pp.2455-2460, 1998.

41. S. A. Bernard, B. M. Jones, and M. Buist, Experience with Prolonged Induced Hypothermia in Severe Head Injury, *Critical Care*, vol.3, pp.167-172, 1999.
42. I. Virkkunen, A. Yli-Hankala, and T. Silfvast, Induction of Therapeutic Hypothermia after Cardiac Arrest in Pre-hospital Patients Using Ice-Cold Ringer's Solution: A Pilot Study, *Resuscitation*, vol.62(3), pp.299-302, 2004.
43. T. Shiozaki, H. Sugimoto, M. Taneda, H. Yoshida, A. Iwai, T. Yoshioka, and T. Sugimoto, Effect of Mild Hypothermia on Uncontrollable Intracranial Hypertension after Severe Head Injury, *Journal of Neurosurgery*, vol.79, pp.363-368, 1993.
44. C. Diao, and L. Zhu, Temperature Distribution and Blood Perfusion Response in Rat Brain During Selective Brain Cooling, *Medical Physics*, vol. 33(7), pp.2565-2573, 2006.
45. Y. Wang, and L. Zhu, Selective Brain Hypothermia Induced by an Interstitial Cooling Device in Human Neck: Theoretical Analyses, *Eur. J. Applied Physiology*, vol.101(1), pp.31-40, 2007.
46. E. Bering, Effect of Body Temperature Change on Cerebral Oxygen Consumption of the Intact Monkey, *American Journal of Physiology*, vol.200, pp.417- 419, 1961.